# Quantifying the role of geographic change in Cenozoic ocean heat transport using uncoupled atmosphere and ocean models

**4 authors**, including:

Christopher Robert Scotese
Northwestern University
**778** PUBLICATIONS   **12,683** CITATIONS

SEE PROFILE

Dan Seidov
National Oceanic and Atmospheric Administration
**125** PUBLICATIONS   **3,747** CITATIONS

SEE PROFILE

Some of the authors of this publication are also working on these related projects:

Project    GODAR Project View project

Project    Northwest Atlantic Ocean Regional Climatology http://www.nodc.noaa.gov/OC5/regional_climate/nwa-climate/ View project

# Quantifying the role of geographic change in Cenozoic ocean heat transport using uncoupled atmosphere and ocean models

Karen L. Bice [a],*, Christopher R. Scotese [b], Dan Seidov [c], Eric J. Barron [c]

[a] *Department of Geology and Geophysics, Woods Hole Oceanographic Institution, Woods Hole, MA 02543-1541, USA*
[b] *Department of Geology, University of Texas at Arlington, Arlington, TX 76019, USA*
[c] *EMS Environment Institute, Pennsylvania State University, University Park, PA 16802, USA*

## Abstract

A series of five Cenozoic atmospheric general circulation model (AGCM) experiments has been performed using a new set of paleogeographic reconstructions for 55, 40, 33, 20 and 14 Ma. The five continental reconstructions incorporate the tectonic evolution of early Eocene to middle Miocene continental positions and topography. With all other model boundary conditions and forcings held constant, the series of AGCM experiments captures a $<1°C$ decrease in annual mean temperature through the Paleogene and early Neogene. Regional and seasonal differences among the five experiments are small in magnitude, but are consistent with the imposed paleogeographic changes. From the AGCM experiments alone, it might be concluded that changes in continental positions had little impact on Cenozoic climate change. However, ocean configuration changes between 55 and 14 Ma, especially gateway openings and closures, are expected to produce significant changes in ocean thermohaline circulation, a system that cannot be simulated by the slab ocean model component of an AGCM. The nature of changes in ocean heat transport and thermohaline circulation arising from the evolution of early Eocene through middle Miocene ocean basin configurations is examined in a series of five global, three-dimensional ocean model experiments forced by output from the AGCM. The ocean model suggests that paleogeographic change throughout the Cenozoic has caused changes in the interhemispheric partitioning of heat transport and that the modern shape of the ocean heat transport curve has evolved in response to ocean basin evolution. The prediction of very low ocean heat transport in the Northern Hemisphere of the early and middle Eocene suggests a much more important role for atmospheric heat transport in the temperate polar climates of the Eocene than is generally acknowledged. Results suggest that Southern Hemisphere ocean heat transport decreased throughout the interval 55–14 Ma. The results also show that, in the absence of reliable coupled models for paleoclimate studies, full three-dimensional ocean models must be used in parallel with slab ocean AGCMs if we wish to understand the true effects of paleogeographic change on climate and the true nature of past ocean heat transport. © 2000 Elsevier Science B.V. All rights reserved.

*Keywords:* Cenozoic; Eocene; modeling; ocean circulation; paleoclimatology; paleogeography

* Corresponding author. Fax: +1-508 457 2187.
*E-mail addresses:* kbice@whoi.edu (K.L. Bice), cscotese@anet-dfw.com (C.R. Scotese), dseidov@essc.psu.edu (D. Seidov), eric@essc.psu.edu (E.J. Barron)

## 1. Introduction

Decreasing high latitude surface and deep ocean temperatures during the early Eocene through Pliocene interval are well-documented by both continental and marine records. Foraminiferal isotopic data indicate that high-latitude surface waters and global bottom waters have cooled from ~12–14°C in the early Eocene to near −2°C today (Shackleton and Kennett, 1975; Douglas and Woodruff, 1981; Miller et al., 1987; Askin, 1991). If small continental ice-sheets were present on Antarctica in the warm early Paleogene, they did not extend to the coastline (Mackensen and Ehrmann, 1992; Zachos et al., 1993). By the early Oligocene, an extensive ice-sheet existed on Antarctica, which subsequently waxed and waned (Zachos et al., 1993). Benthic and planktonic foraminiferal $\delta^{18}O$ values have diverged since the early Oligocene, reflecting the development of a thermally well-stratified ocean (Douglas and Savin, 1975; Shackleton et al., 1984). Global sea level height, relative to the modern, has undergone an overall decrease since the late Cretaceous, reflecting a combination of decreased global ocean ridge volume, ice-sheet construction, and thermal contraction of sea water with cooling (Vail et al., 1977; Kominz, 1984; Haq et al., 1987).

The two mechanisms commonly used to explain the long-term Cenozoic cooling trend are a gradual decrease in atmospheric $CO_2$ partial pressure and changing geography. Ice-sheets of some size have also contributed to cooling through an ice–albedo–temperature positive feedback forcing. However, the initial expansion of Antarctic ice was most likely a response to polar or global cooling, not a forcing itself (Robin, 1988).

Considerable uncertainty exists in the reconstruction of past carbon dioxide concentrations. An overall decrease in $CO_2$ is supported by carbon cycle models and by limited data (Freeman and Hayes, 1992; Berner, 1994). However, recent work indicates plausible atmospheric carbon dioxide levels similar to or lower than the modern during intervals believed to have been warmer than the present-day (Cowling, 1999; Flower, 1999; Pagani et al., 1999; Pearson and Palmer, 1999). With debate over past carbon dioxide concentrations and uncertainty in the true response of the climate system to changes in radiative gas levels, it becomes more important to attempt to isolate the role of paleogeographic change in the long-term climate signal. Numerous studies address the potential impact of Cenozoic plate tectonics on climate trends through the carbon cycle [Raymo et al., 1988; Raymo, 1991; Edmond, 1992; Raymo and Ruddiman, 1992; Reusch and Maasch, 1998; Beck et al., 1999; see also the many papers cited in Ruddiman (1997)] and through air mass changes with mountain uplift (Ruddiman and Kutzbach, 1990; Broccoli and Manabe, 1992; Kutzbach et al., 1993; Otto-Bliesner, 1998). The present study focuses on the role of paleogeographic change alone in determining long-term changes in poleward heat transport and global ocean thermohaline circulation.

Several studies have attempted to quantify the effects of changing geography and atmospheric composition using numerical models. Early planetary albedo considerations by Barron (1981) suggested that paleogeographic evolution of the past 100 million years operated in the correct sense and approximately correct order of magnitude to explain the Mesozoic-to-recent cooling trend. However, experiments using several generations of NCAR general circulation models (GCMs) (Barron and Washington, 1982, 1984; Barron et al., 1984, 1989; Barron, 1985, 1989) indicate that an additional climate forcing parameter, most likely carbon dioxide, is necessary to explain the Tertiary cooling trend. A fundamental modeling problem that persists is that reconstructed paleogeography and elevated carbon dioxide together still fail to reproduce the pole-to-equator temperature profiles inferred from isotopic data for the Mesozoic and early Tertiary.

Greater than modern ocean heat transport is a frequently cited explanation for high-latitude warmth in the early Cenozoic (Covey and Barron, 1988; Rind and Chandler, 1991; Barron et al., 1993; Sloan and Rea, 1995), implying that decreased ocean heat transport from the Eocene to the present might help explain high latitude (and therefore deep ocean) cooling. Model studies that include a parameterization meant to represent increased ocean heat transport do a better job of

simulating inferred meridional paleotemperature gradients (Barron et al., 1993, 1995; Sloan and Rea, 1995). However, no known physical mechanism exists to justify ocean heat transport greater than the modern (Sloan et al., 1995), especially at times when the oceanic thermal gradients were significantly reduced relative to the modern (Bice and Marotzke, 1999).

The magnitude of ocean heat transport in the Cenozoic is entirely unconstrained by data, and numerical models are therefore the best tool for understanding the true nature of ocean heat transport and how it may have changed through the Cenozoic. An important boundary condition that atmospheric GCMs cannot incorporate is the role of the three-dimensional ocean circulation, a condition largely determined by paleogeography. Seidov (1986) made the first attempt to reconstruct long-term changes in ocean circulation using a numerical ocean model and a realistic progression of changes in basin geometry. These experiments illustrated sensitivity of the circulation and the resulting temperature distribution to tectonic evolution and captured several trends consistent with paleoceanographic data-based reconstructions. However, Seidov (1986) was unable to explain the high-latitude and deep-water warmth of the Cretaceous and early Cenozoic using paleogeographic changes alone.

Other numerical studies have examined the influence of changes in individual gateways and seafloor topographic features. Maier-Reimer et al. (1990) investigated the effect of an open central American passageway, a condition appropriate for $\sim 4$ Ma. Surface transport through the open gateway resulted in a surface salinity variation effective in significantly decreasing deep water production in the North Atlantic basin. Mikolajewicz et al. (1993) showed that a closed Drake Passage (appropriate prior to $\sim 38$ Ma) increased bottom water production rates in the South Ocean, which in turn decreased the rate of North Atlantic deep water production, in agreement with simulations that used highly idealized modern geometries (Gill and Bryan, 1971; Cox, 1989; England, 1992; Toggweiler and Samuels, 1993).

The first part of the present study is an atmospheric model study with a slab ocean component.

As in the work of Barron (1985) and a subset of the experiments described by Fawcett and Barron (1998), the objective is to isolate the role of paleogeographic evolution in the Cenozoic climate trend. We focus, however, on the resulting changes in ocean heat transport. We use a more recent, higher-resolution atmospheric GCM than was used in earlier studies. Five Cenozoic atmospheric model experiments were performed using a new set of paleogeographic reconstructions for early Eocene ($\sim 55$ Ma), middle Eocene ($\sim 40$ Ma), early Oligocene ($\sim 33$ Ma), early Miocene ($\sim 20$ Ma), and middle Miocene ($\sim 14$ Ma) (Scotese et al., 1998). These intervals were chosen in order to bracket important changes in ocean basin configuration. The five reconstructions incorporate widening of the Atlantic and Southern Ocean basins, widening of Drake Passage and separation of the South Tasman Rise from Antarctica, collision of India with Asia, narrowing and closure of the eastern Tethys, northward movement of Australia, narrowing of the Indonesian–Pacific and Central American passageways, and widening of the North Atlantic. The evolution of continental elevations reflects primarily the northward movement and rise of the Andes belt, uplift of the Himalayas and Tibetan Plateau, and the increase in land fraction and elevation in the northern tropics with the closure of the Tethyan Seaway (Table 1).

In the second part of this study, we use the atmospheric general circulation model (AGCM) output to force full three-dimensional ocean-only experiments with ocean basin reconstructions corresponding to the five AGCM paleogeographies. This allows us to explore further the possible changes in the role of the ocean in long-term Cenozoic climate change and to examine potential pitfalls in inferring heat transport partitioning using a slab ocean GCM alone. The series of atmosphere and ocean model runs are single variable sensitivity tests in which the objective is not to reconstruct every boundary condition for the geologic interval, but to examine the role of continental and ocean basin configurations alone. It must be noted that single variable sensitivity tests using uncoupled atmosphere and ocean models allows us to examine only fundamental, large-scale

Table 1
Continental areas ($10^6$ km$^2$) for the five Cenozoic reconstructions

|  | Total | SH | NH | 13°–33°N |
|---|---|---|---|---|
| Early Eocene (∼55 Ma) | 146.7 | 55.6 | 91.1 | 21.0 |
| Middle Eocene (∼40 Ma) | 136.9 | 44.9 | 92.0 | 23.0 |
| Early Oligocene (∼33 Ma) | 142.7 | 44.7 | 98.0 | 27.6 |
| Early Miocene (∼20 Ma) | 142.0 | 44.9 | 97.1 | 29.2 |
| Middle Miocene (∼14 Ma) | 151.2 | 47.1 | 104.1 | 30.4 |

responses of ocean circulation to the boundary condition varied.

## 2. Atmospheric model experiments

The GENESIS v. 2.0.a atmospheric model (Thompson and Pollard, 1997) consists of a global spectral atmospheric model with 18 layers, coupled to multi-layer vegetation, soil, and snow models, and a 50 m slab ocean model. A triangular 31-wave spectral truncation is used for the atmospheric model component, yielding a transform grid resolution of approximately 3.75° × 3.75°. An independent, 2° resolution surface grid is used for the land-surface transfer components (vegetation, soil, ocean, etc.). Paleogeography is specified to the model at 2° resolution. As the model runs, at each time step, a simple correction is applied to the lowest level meteorological fields of the spectral atmospheric model, over all surface types, in order to correct for differences between the spectral topography (the T31 truncation) and the 'true' topography (the 2° reconstruction) before calculations are made in the land-surface model components. Ocean heat transport is modeled as linear diffusion down the local temperature gradient, calculated at each time step. Diffusion coefficients in the slab ocean model are a function of the sea surface temperature (SST) gradient, latitude, and the zonal fraction of land at each latitude.

Five simulations were run, each with a different geography, but with all other model parameters held constant. Atmospheric $CO_2$ and $CH_4$ concentrations were fixed at values used in modern 'control' experiments (345 ppm and 1.6 ppm respectively). Solar insolation and orbital parameters were held constant at modern control values.

A globally uniform, mixed vegetation was specified. No continental ice-sheets were prescribed for any paleogeography. No scaling was used to imply increased or decreased heat transport. GENESIS simulations were executed for 20 model years. Averages discussed below are based on the last 5 years of steady-state model output.

Both seasonal and mean annual climate statistics show that the five simulations differ little. Consistent with earlier model studies (Barron, 1985; Fawcett and Barron, 1998), the GENESIS model supports the theory that paleogeography alone does not explain the Cenozoic cooling trend. The evolution of global (Fig. 1a) and hemispheric (Fig. 1b and c) averages of mean annual surface temperature (combined land and ocean) show, however, that the experiment does reproduce a small surface cooling trend. On a global average basis, the annual surface temperature cools by less than 1°C, from 16.4 to 15.8°C. The cooling occurs primarily in the Northern Hemisphere (Fig. 1b), where the average temperature decreases from 16.3°C at 55 Ma to 15.2°C for the 14 Ma reconstruction. The simulated Southern Hemisphere surface temperatures (combined land and ocean) are approximately constant with time (Fig. 1c).

The global mean surface temperatures are approximately equal to those obtained by Fawcett and Barron (1998) for 60, 40 and 20 Ma simulations using the GENESIS v. 1.02 model. In addition, a small (3 cm yr$^{-1}$) overall decrease in global mean precipitation rate with decreasing mean surface temperature is observed, in agreement with the results of Fawcett and Barron (1998). However, the predicted mean precipitation rates are much smaller than those obtained for the Cenozoic using the GENESIS v. 1.02 model. In the present study, global mean precipitation ranges
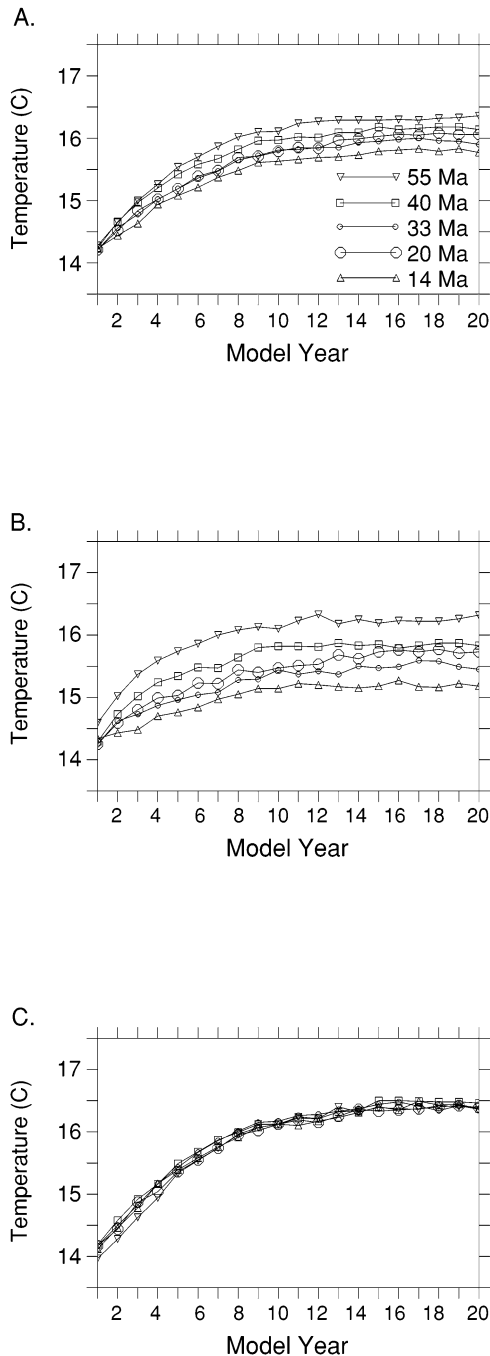
A.



B.



C.



Fig. 1. Time series of model annual surface temperature (averaged over all surface types) during 20-year experiments: (a) global mean; (b) northern hemisphere mean;, (c) southern hemisphere mean.

from 116 to 119 cm yr$^{-1}$, whereas Fawcett and Barron (1998) obtained values of 164–168 cm yr$^{-1}$. This change in global precipitation is the result of a corrected roughness length value for surface heat and water vapor fluxes over ocean in the newer GENESIS model version. The predicted changes in local moisture fluxes are consistent with those described by Fawcett and Barron (1998) and are attributed to continental plate motions through climate belts. For example, North Africa and India become drier through the Cenozoic (Fig. 2), as they move northward out of the influence of the Intertropical Convergence Zone. On a mean annual basis, Australia becomes drier in the Miocene, as it moves northward into the Southern Hemisphere semi-arid latitudes.

Surface temperatures averaged over land only show no clear temporal trend in either hemisphere, although local temperature changes due to changes in latitude and in elevation are observed, with cooling over northern Africa and Asia, for example. Decreases in ocean surface temperatures account for all of the cooling in both hemispheres, and this effect is most pronounced in the Northern Hemisphere (Fig. 3), primarily over the North Atlantic and Tethyan Ocean basins. Warmer Atlantic surface temperatures in the 55 Ma case are primarily due to increased latent heating in response to greater ocean area in the net evaporative latitudes (Table 1). They may also be due in part to greater atmospheric heat convergence over the western North Atlantic basin in response to a well-defined stationary wave trough caused by high orography specified in western North America for 55 Ma. Regional elevations are reduced slightly in the younger geographies, and Atlantic region atmospheric transport decreases. A 3000 m elevation for the northern Eocene Rocky Mountains is based on the results of Norris et al. (1996), who found evidence for seasonal runoff of isotopically depleted freshwater in Green River lacustrine deposits and, therefore, inferred snowfall at high elevations during the warm early Eocene. However, given the large uncertainty in reconstruction of elevations (Ziegler et al., 1997), the component of cooling resulting from North America orographic changes imposed here might be consid-
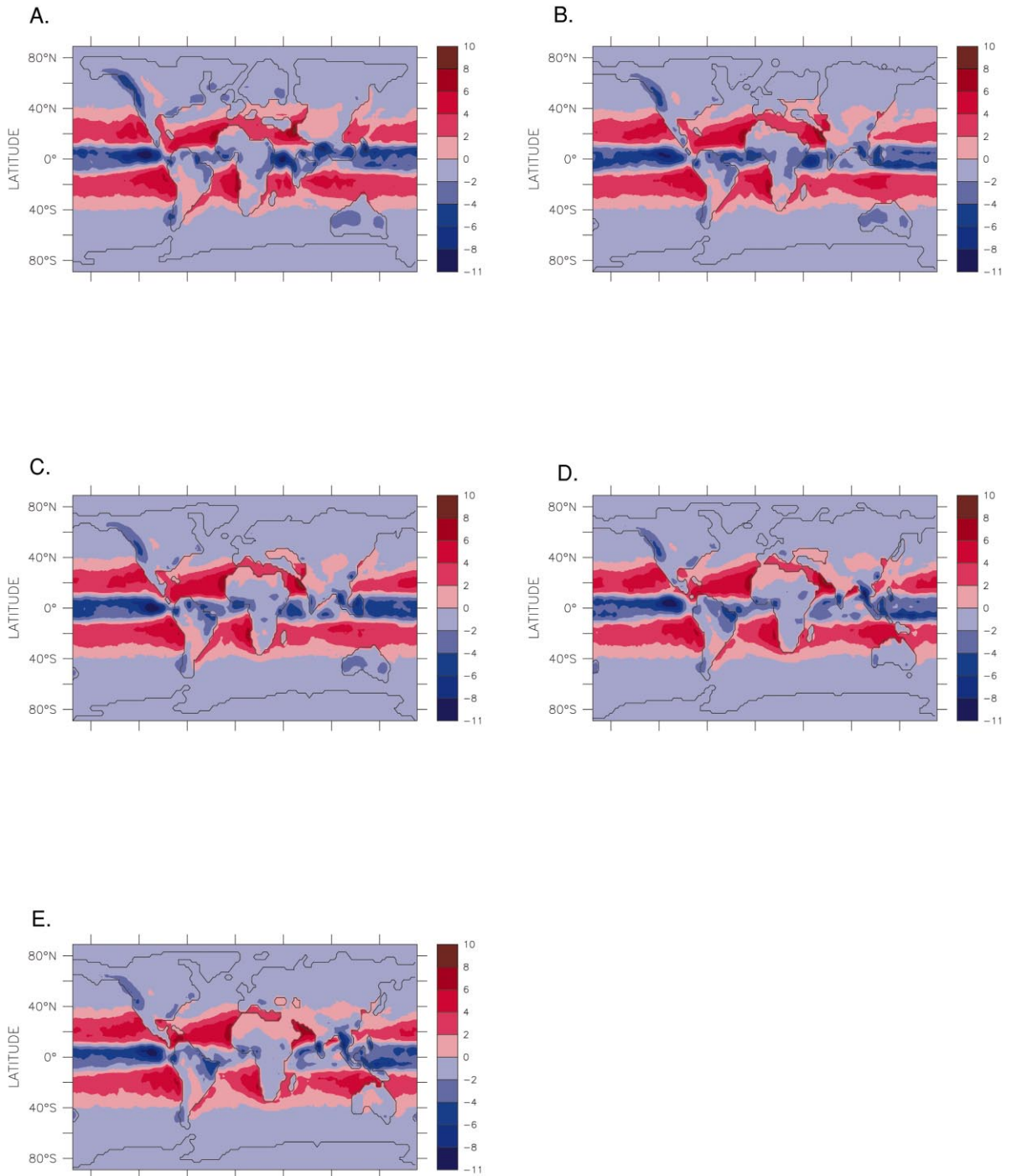
A.

B.

C.

D.

E.

Fig. 2. Model-predicted moisture flux (evaporation minus precipitation) in $10^6$ cm s$^{-1}$: (a) 55 Ma; (b) 40 Ma; (c) 33 Ma; (d) 20 Ma; (e) 14 Ma.
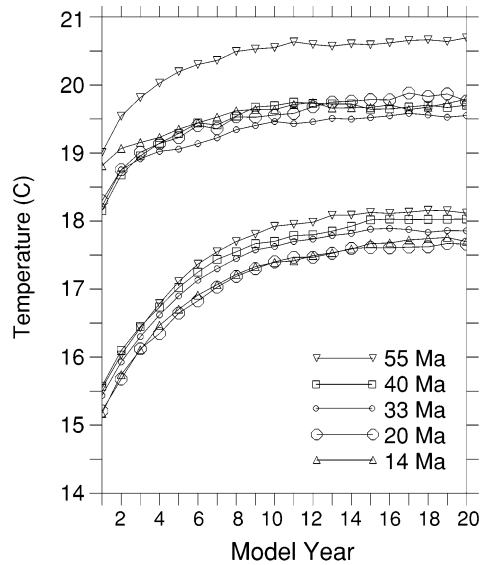
Fig. 3. Time series of model annual surface temperature (averaged over ocean only) for Northern Hemisphere ocean (upper curves) and Southern Hemisphere ocean (lower curves).

ered to be within the error in the model result due to uncertainty in that boundary condition.

The zonal, mean annual surface climate conditions vary little among the five simulations (Fig. 4). The Northern Hemisphere ocean temperature differences are expressed in the zonal profiles (Fig. 4a) between approximately 40° and 70°N. Zonal surface wind stresses over ocean (Fig. 4b) are reduced in the Northern Hemisphere westerlies for the 55 Ma case. The cause of this reduction is not clear, but it may correlate in part with a small reduction in the meridional temperature gradient between 35° and 50°N in the Atlantic/Tethyan basins in the 55 Ma case. However, the temperature gradient decrease is small, and although the gradient increases gradually between the 55 and 14 Ma cases, simulated Northern Hemisphere wind stresses increase abruptly from the 55 to 40 Ma case.

Consistent with earlier experiments (Barron and Washington, 1984; Sloan and Barron, 1990; Crowley, 1993), the warm polar conditions of the early Cenozoic are not reproduced by specifying paleogeography alone. In comparison with a reconstruction of Southern Ocean SSTs based on planktonic foraminifera from ODP Sites 690 and
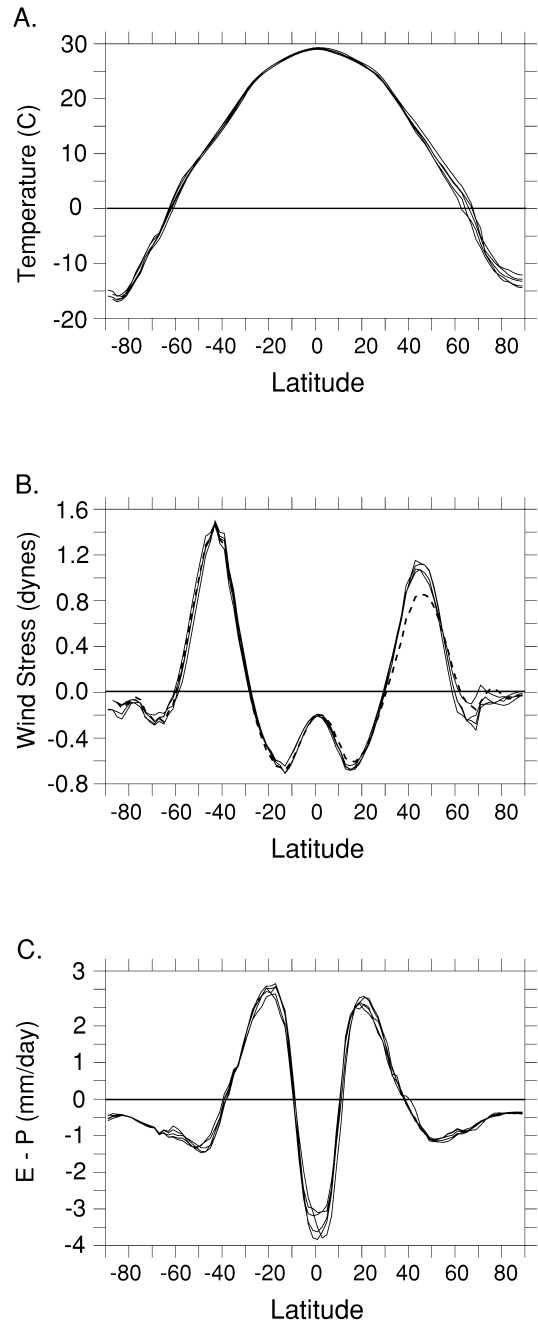


Fig. 4. Zonal mean annual climate conditions predicted by the AGCM: (a) surface temperature (°C); (b) eastward wind stress (dynes) averaged over ocean only; (c) evaporation minus precipitation (millimeters per day) averaged over all surface types. Because they nearly coincide, curves for all five cases are plotted using the same line type, with the exception of the wind stress profile for 55 Ma, which is dashed.

738 ($\sim 17°C$ at 62–65°S) (Stott et al., 1990; Barrera and Huber, 1991), the early Eocene temperature is under-predicted by $\sim 15°$, and sea-ice is simulated at Site 690 in winter months. In comparison, simulated mean annual surface temperatures at Walvis Ridge are within 1°C of those inferred from early Eocene planktonic foraminifera ($\sim 18°C$ at 33°S paleolatitude).

The failure of AGCMs to simulate the reduced pole-to-equator gradients of warm climate intervals is a long-standing problem in paleoclimate modeling. As was discussed above, a combination of increased radiative gas forcing and increased ocean heat transport (relative to the modern control magnitude) has been used to produce reasonable matches to temperatures inferred from climate records. However, no known mechanism exists for increasing ocean heat transport at a time when meridional surface temperature and vertical temperature gradients were greatly reduced relative to the modern (Sloan et al., 1995; Bice and Marotzke, 1999).

## 3. Ocean heat transport implied by the slab ocean model

The total (atmosphere plus ocean) poleward annual heat transport, calculated from the net downward radiative flux at the top of the model atmosphere does not differ among the five AGCM runs (Fig. 5a). This is to be expected, given that

all forcing parameters except geography are held constant and no appreciable changes in mean annual cloudiness and snow cover are predicted among the five cases. The ocean heat transport, calculated from the heat convergence in the slab ocean model due to the diffusive transport parameterization, also does not vary significantly (Fig. 5b). This is not a surprising conclusion from the perspective of a fixed-depth slab ocean in which heat transport is parameterized as a function of surface temperature (which does not vary appreciably among these runs) and ocean fraction at each latitude. A comparison of the latitudinal distribution of ocean area in the two end-member geographies (55 and 14 Ma) is shown in Fig. 6. Small differences among the implied ocean heat transport curves correlate with ocean area differences in the five paleogeographic reconstructions. For example,
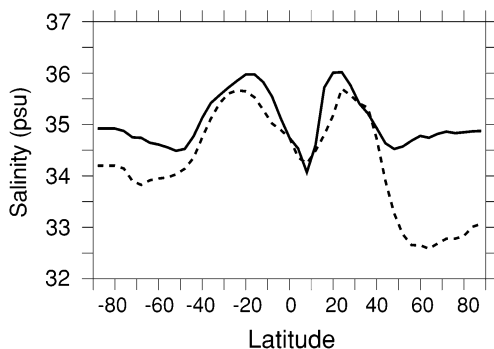


Fig. 5. Zonal mean annual surface salinity from Levitus et al. (1994) (dashed line) and that derived from the moisture flux of an unpublished GENESIS modern simulation (solid line).
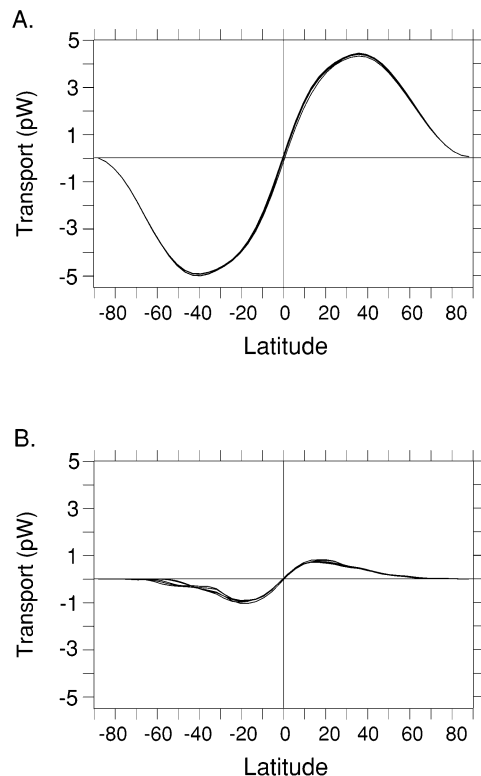


Fig. 6. Northward heat transport (petawatts) implied by the AGCM: (a) atmosphere plus ocean; (b) slab ocean only. Because they nearly coincide, curves for all five cases are plotted using the same line type.

as ocean area between 40°and 65°S latitude increases from 55 to 14 Ma, the implied poleward ocean heat transport increases in these latitudes. A similar relationship is observed between ~15°and 35°N: ocean area decreases as the Tethyan Seaway closes, and the implied heat transport at these latitudes decreases. However, the differences in implied ocean heat transport among the five AGCM runs are small and, viewed on the scale of the total transport, the curves are nearly identical (Fig. 5b). Like the total (atmosphere plus ocean) heat transport (Fig. 5a), the implied ocean heat transport is largely symmetric about the equator, with no net transport between hemispheres simulated by the model.

## 4. Global ocean model experiments

The performance of uncoupled ocean experiments allows a comparison between the heat transport implied by the slab ocean diffusion in the AGCM and that calculated using a full three-dimensional ocean forced by the AGCM output. In order to examine the evolution of ocean heat transport attributable to basin configuration and gateway changes alone, five simplified paleobathymetries were constructed, corresponding to the five paleogeographic reconstructions of the AGCM runs. Simplified basin reconstructions are consistent with the 2° resolution continental positions specified to GENESIS, and ocean depths were specified as either shallow (500 m) or deep (5150 m). The major basin changes captured by the reconstructions are summarized in Table 2. As part of the required shoreline smoothing, the

Arctic Ocean was removed in all experiments and the maximum poleward extent of ocean area was set at 74°N and 86°S. In the 14 Ma basin configuration, the Mediterranean Sea was removed owing to the inability to resolve flow there using 4° horizontal resolution.

Zonally averaged, mean annual temperature and surface wind stress over ocean were calculated directly from the GENESIS model output (Fig. 4a and b) to generate ocean surface forcing. Minimum surface forcing temperatures were set to $-2°C$. Surface salinity forcing was derived by first calculating zonal mean annual evaporation minus precipitation rate $(E-P)$ (Fig. 4c) over all model surface types (ocean and land). This allows the inclusion, in a crude manner, of net precipitation that would be in the form of continental runoff (Bice et al., 1997). $E-P$ was converted to a salt flux using a modified version of the equation of Weaver et al. (1994):

$$Q_S = \rho_0 S_0 \times (E-P),$$

where $\rho_0$ is sea water density and $S_0$ is the constant reference salinity (35 psu). In a modern GENESIS experiment, when this salt flux is converted to a surface salinity, the model produces a fair match to the zonal mean annual surface salinity calculated from the observations of Levitus et al., 1994 (Fig. 7).

Forcing derived from the AGCM was applied to the GFDL Modular Ocean Model v. 1.0 (Pacanowski et al., 1993). The model configuration specified is 4°horizontal resolution and 16 vertical layers. Upper ocean layer temperatures were relaxed toward specified forcing values using Newtonian damping with a restoring time scale of

Table 2
Basin configurations specified to the ocean model

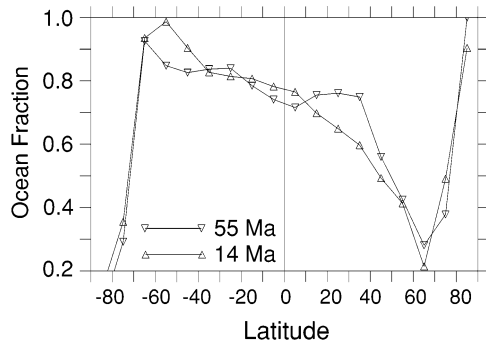| | |
|---|---|
| Early Eocene (~55 Ma) | India–Asia gateway open; Drake and Australia–Antarctic gateways closed; Eastern Mediterranean open; Central American passageway open. |
| Middle Eocene (~40 Ma) | India–Asia gateway closed; Australia–Antarctic gateway open; Atlantic widening; Tethys narrowing. |
| Early Oligocene (~33 Ma) | Drake Passage open; Australia–Antarctic passageway widening; Tethys narrowing. |
| Early Miocene (~20 Ma) | Southern Ocean widening; Atlantic widening; Tethys narrowing. |
| Middle Miocene (~14 Ma) | Eastern Mediterranean closed; Southern Ocean wide; Atlantic wide; Central American passageway open; Indonesian–Pacific gateway narrow. |

Fig. 7. Ocean fraction as a function of latitude for the 55 Ma and 14 Ma geographies.



Fig. 8. Northward ocean heat transport (petawatts) simulated by the global ocean model.

50 days. Constant horizontal and vertical sub-grid scale mixing coefficients were specified. Ocean experiments were run for 5000 model years to reach steady state in the thermohaline circulation.

The simplified configurations used here (relatively coarse resolution, zonal mean surface forcings with no seasonal cycle, simplified treatment of continental runoff) are not meant to be realistic representations of the atmospheric systems. However, they are consistent with the most recently available paleogeographic reconstructions and they allow the performance of single-variable sensitivity tests. Similar mean annual zonal forcing techniques have been applied by others in examining the gross features of the modern thermohaline circulation (Gill and Bryan, 1971; Cox, 1989; England, 1992; Stocker et al., 1992). As was stated earlier, the absence of an ocean-atmosphere feedback in the uncoupled modeling approach allows us to look at only large-scale responses of ocean circulation to changes in ocean basin configuration. Important feedbacks, especially those involving changes in moisture flux and ocean-atmosphere heat fluxes, are not a part of this type of study and, in the absence of a well-tested coupled paleoclimate model, require a different type of sensitivity test (Bice et al., 1997).

## 5. Ocean heat transport calculated from the global ocean model

In comparison to the heat transport implied by the slab ocean parameterization, which varied little
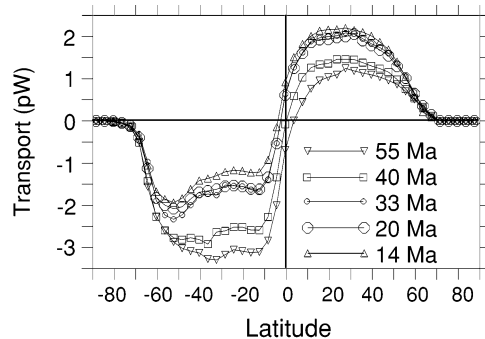
among the five AGCM runs (Fig. 5b), there are substantial differences in the magnitude of heat transport among the five ocean model experiments (Fig. 8) and an intriguing trend is apparent. Given zonal, mean annual atmospheric forcings predicted by the AGCM, from 55 to 14 Ma, the model predicts an overall decrease in Southern Hemisphere transport and an increase in Northern Hemisphere transport. Because the atmospheric forcings applied to the five basin configurations are nearly identical (Fig. 4), the evolution of the calculated ocean heat transport (Fig. 8) and meridional overturning (Fig. 9) occurs primarily in response to ocean basin evolution.

In the modern system, maximum ocean heat transport is estimated to be 0.2 to 1 PW greater in the Northern Hemisphere (Hastenrath, 1982; Carissimo et al., 1985). In contrast, the Eocene paleogeographies result in much higher heat transport in the Southern Hemisphere oceans than in the northern. The older basin configurations (55 and 40 Ma) exhibit large Southern Hemisphere overturning gyres (Fig. 9a and b) and high southward heat transport. These result from the existence of continuous or nearly continuous continental barriers that support southward upper ocean boundary current flow and a large northward return flow in the deep boundary system. In these same reconstructions, the existence of a through-going low latitude Northern Hemisphere pathway for warm equatorial waters results in low poleward heat transport in the Northern Hemisphere. Warm equatorial waters are not
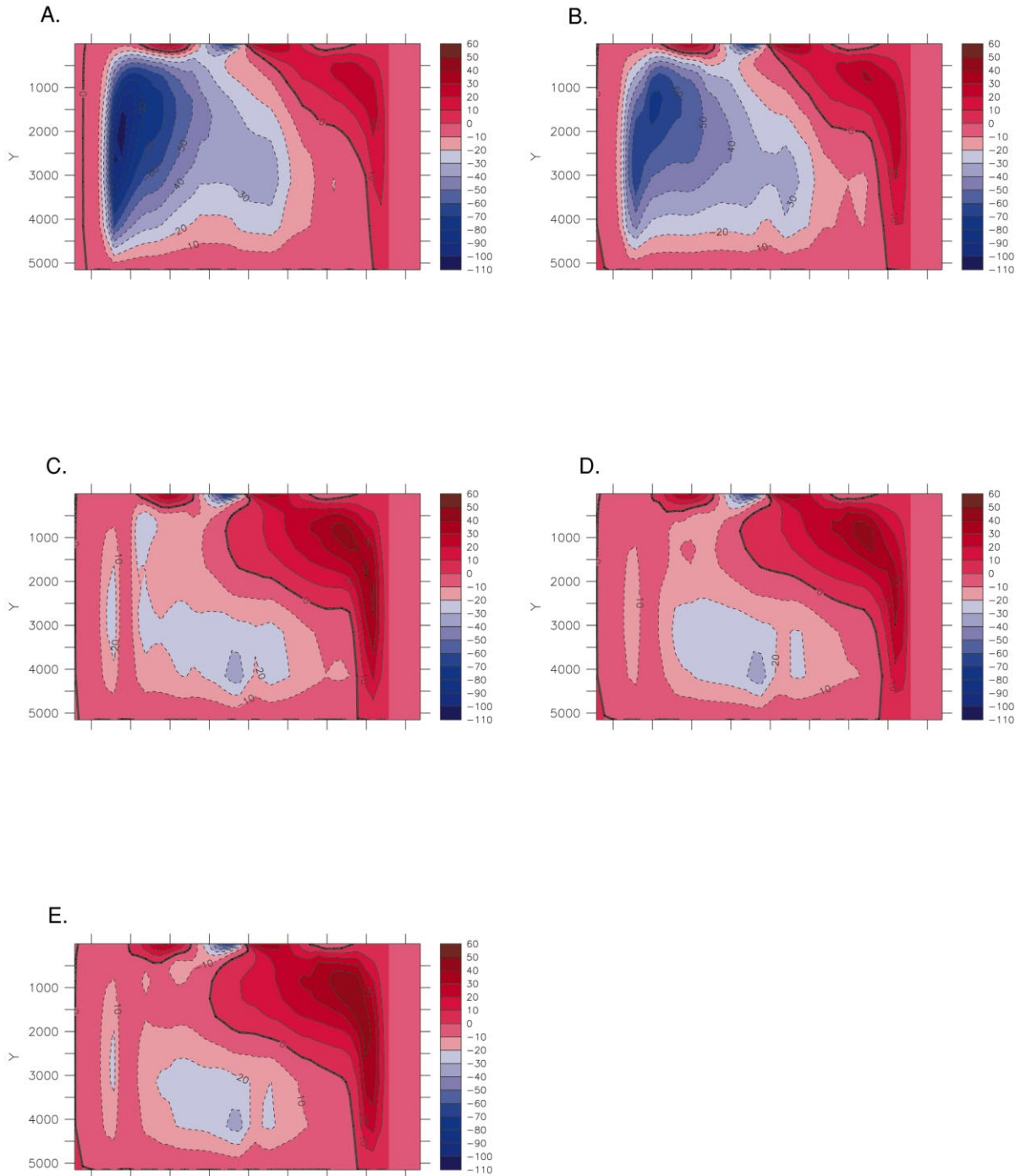
Fig. 9. Meridional overturning (Sverdrups; $1 \text{ Sv} = 10^6 \text{ m}^3 \text{ s}^{-1}$) simulated by the global ocean model: (a) 55 Ma; (b) 40 Ma; (c) 33 Ma; (d) 20 Ma; (e) 14 Ma.

diverted poleward in the Northern Hemisphere. Numerous additional ocean model runs have been performed using the early Eocene (55 Ma) basin configuration and a variety of atmospheric forcings, including that used to force the middle Miocene (14 Ma) experiment described here. The pronounced asymmetry in early Eocene ocean heat transport and meridional overturning shown in Figs. 8 and 9 is supported by all these additional experiments, indicating that the response is primarily due to basin configuration, not surface forcing.

As the Southern Ocean gateways evolve and widen, lower overturning is supported in the Southern Hemisphere and heat transport there decreases. Meanwhile in the Northern Hemisphere, the creation of barriers to flow (India–Asia collision, eastern Mediterranean closure) and narrowing gateways (Tethyan, Central American, Indonesian–Pacific) divert warm equatorial currents poleward and allow the development of strong boundary current transport and an increase in meridional overturning in the Northern Hemisphere (Fig. 9c–e). Thermohaline overturning in the North Atlantic basin strengthens as the basin geometries evolve from 55 to 14 Ma. This occurs in response to a number of geographic changes: decreased outflow of Southern Hemisphere ('proto-AABW') deep water with the breakdown of southern ocean barriers in the Drake Passage and Tasman region (Mikolajewicz et al., 1993), closure of mid- and low-latitude gateways, and opening of the far North Atlantic basins. Little change in transport occurs between the 33 Ma and 20 Ma case because no new gateway opening or closure was specified in the 20 Ma configuration (Table 2). A configuration intermediate to the 40 and 33 Ma cases (not shown), in which Drake Passage was open to surface flow but included a 500 m deep sill, yielded ocean heat transport that was intermediate to that shown for the 40 and 33 Ma cases.

A similar uncoupled experiment was performed using a 4° resolution version of the modern ocean configuration. Unlike the five Eocene through Miocene experiments described so far, this 'modern' run was not a single variable sensitivity test, and it is not described in detail here. However, the heat transport predicted by the ocean model in the 'modern' case continues the trend observed in the 55–14 Ma runs: Northern Hemisphere overturning and heat transport show further increases with the closure of the central American passageway and narrowing of the Indo-Pacific gateway. The total ocean heat transport resembles that estimated for the modern ocean from a variety of sources (Trenberth, 1979; Hastenrath, 1982; Carissimo et al., 1985). As in the estimates of Hastenrath (1982) and Carissimo et al. (1985), the 'modern' case exhibits slightly greater maximum transport in the Northern Hemisphere than in the Southern Hemisphere, with maximum northward transport of 2.6 PW at 26–32°N, a value between the estimates of Hastenrath (1982) and Carissimo et al. (1985). The Southern Hemisphere maximum transport (1.6 PW) nearly equals that of Trenberth (1979), whose estimate (1.7 PW) was lower than that of Hastenrath (1982) and Carissimo et al. (1985).

The predicted long-term evolution of the ocean heat transport includes the change from net transport southward across the equator in the 55 Ma case to a small net northward cross-equatorial transport in the 'modern' case, a condition similar to some modern estimates (Hastenrath, 1982).

## 6. Discussion

The global mean surface temperature predicted for the five AGCM experiments varies within less than 1°C. This is because the global mean temperature is determined primarily by solar insolation, mean albedo and the radiative effects of the atmosphere. The solar constant is unchanged among these experiments, and mean albedo varies very little with the specified paleogeographic changes and with no ice-sheets specified in any of the configurations. A somewhat greater greenhouse effect is simulated for the Eocene configurations with the existence of the Tethys Seaway, but the temperature effect is less than 10% of the maximum Cenozoic cooling inferred from proxy data.

The strong asymmetry in the Eocene ocean heat transport (Fig. 8) has also been simulated using a different ocean model, higher vertical and horizontal resolution, full two-dimensional, full sea-

sonal-cycle forcing, and a bathymetric reconstruction with realistic bottom topography (Bice, 1997). That, along with the evolution of the ocean heat transport profiles observed here, suggests that ocean heat transport has not always been largely equal in both hemispheres. It seems reasonable that this asymmetry may have been a feature of paleogeographies quite different from the modern, such as the mid-Silurian (∼425 Ma), for example, when the continents were distributed so that there was largely an oceanic Northern Hemisphere and a continental Southern Hemisphere (Scotese and McKerrow, 1990). In the mid-Silurian Southern Hemisphere, only the atmosphere could have transported energy between 60° and 90°S. The ocean model results described here indicate that the implied symmetrical heat transport in the AGCM slab ocean is an unrealistic solution in geographies much more recent than the Silurian (early and middle Eocene) and that relatively subtle paleogeographic changes cause changes in the interhemispheric partitioning of heat transport.

If largely non-symmetrical ocean heat transport is a realistic prediction, what does it imply about ancient atmospheric heat transport? The surplus of incoming over outgoing energy can only be transported out of the tropics by the atmosphere and ocean. If ocean heat transport was very low in one hemisphere, the atmosphere must have compensated (Stone, 1978). This implies a very important role for the atmosphere in the Northern Hemisphere of the early Eocene, which may help explain a diverse warm climate macrofaunal assemblage on Ellesmere Island, above 78°N paleolatitude (Estes and Hutchison, 1980; McKenna, 1980) and in a region with poor communication to the global ocean. Increased latent heat transport, above that predicted given the existence of the Tethyan Ocean area in the 55 and 40 Ma paleogeographies, must be considered.

The question of the actual evolution of heat transport partitioning through the Cenozoic is far from answered by these sensitivity tests. One aspect ignored here is the Cenozoic cooling trend itself. How would Cenozoic ocean heat transport evolve when polar cooling from the Eocene to the Miocene is imposed on the ocean model? This is the subject of an ongoing model study. As polar surface waters and the deep ocean cooled from the Eocene to the Miocene, both meridional and vertical gradients in the ocean increased, resulting in an increase in heat transport (Bice and Marotzke, 1999). In the Northern Hemisphere, both basin configuration change and increased temperature gradients cause an increase in ocean heat transport from the early Eocene to the middle Miocene. In determining whether Southern Hemisphere ocean heat transport increased or decreased between 55 and 14 Ma, the question becomes: Is the paleogeographic change that forces a decrease in ocean heat transport more or less important than the thermal gradient increase that forces an increase in transport? Preliminary ocean model results suggest that the decrease in transport due to Southern Hemisphere basin changes is larger than the increase forced by the development of large ocean temperature gradients. This result supports the conclusion from the paleogeography sensitivity experiments that, from 55 Ma to 14 Ma, the Earth has experienced an overall decrease in Southern Hemisphere poleward ocean heat transport and an increase in Northern Hemisphere transport.

The qualitative consideration of the importance of meridional and vertical thermal gradients in the heat transport calculation dictates that the common assumption of higher global ocean heat transport in the warm polar intervals must be incorrect and that the role of the atmosphere during these intervals has been down-played. Attention must be returned to the potential importance of greater latent heat transport during times when plate positions and higher sea levels provided a larger available moisture supply (Barron et al., 1989). For this, it becomes especially critical to define subtropical SSTs for intervals of extreme warmth and establish whether temperatures higher than the modern existed, beyond the ± 2°C uncertainty in the isotopic paleotemperatures (Bice et al., 1999a,b). As long as subtropical SSTs even 2°C warmer than the modern are plausible for the early Eocene, poleward heat transport through the atmosphere should be considered a substantial mechanism for the polar warmth of that interval. Additionally, it is important to identify possible differences in meridional surface paleotemperature

gradients between the two hemispheres. Because of the scarcity of paleotemperature proxy data for many intervals, paleotemperatures are often reconstructed as a function of absolute latitude. This approach can mask interhemispheric differences from which we might better understand warm interval climate processes.

The lack of agreement between the ocean heat transport implied by the AGCM and that calculated from the ocean model highlights a number of difficult questions about the use of slab ocean models in studying paleoclimates. Can realistic ocean heat transport be inferred from a slab ocean, or must it always be specified based on some quantitative understanding of the system that is to be simulated, as is done for the modern? If the ocean heat transport implied by the slab ocean model is unrealistic, is the simulated atmospheric transport of the AGCM reliable? Specifying a heat transport parameterization is a difficult, perhaps impossible, approach for past climate intervals, because it requires knowing the system condition that we hope to predict. At the same time, realistic ocean dynamics cannot be incorporated into an atmospheric model with a slab ocean component. This limitation is a feature of all GCMs, but it does not invalidate the use of the models in performing a wide variety of climate sensitivity tests. However, in attempting to understand the true effects of paleogeographic change on climate or the true nature of ocean heat transport, full three-dimensional ocean models must be used in parallel with slab ocean AGCMs. This will assure that results converge on the most reliable conclusions possible, within the limitations of uncoupled models. The paleoclimate community hopes that fully coupled atmosphere-ocean models will eventually be useful in understanding ancient climate systems, especially intervals of warm polar climates.

## Acknowledgements

## References

Askin, R.A., 1991. Campanian to Paleocene spore and pollen assemblages of Seymour Island, Antarctica. Rev. Palaeobot. Palynol. 65, 105–113.

Barrera, E., Huber, B.T., 1991. Paleogene and Early Neogene oceanography of the southern Indian Ocean: Leg 119 foraminifer stable isotope results. Proc. Ocean Drill. Program Sci. Results 119, 693–717.

Barron, E.J., 1981. Paleogeography as a climatic forcing factor. Geol. Rund. 70, 737–747.

Barron, E.J., 1985. Explanations of the Tertiary global cooling trends. Palaeogeogr. Palaeoclimatol. Palaeoecol. 50, 45–61.

Barron, E.J., 1989. Climate variations and the Appalachians from the late Paleozoic to the present: results from model simulations. Geomorphology 2, 99–118.

Barron, E.J., Washington, W.M., 1982. Cretaceous climate: a comparison of atmospheric simulations with the geologic record. Palaeogeogr. Palaeoclimatol. Palaeoecol. 40, 103–133.

Barron, E.J., Washington, W.M., 1984. The role of geographic variables in explaining paleoclimates, results from Cretaceous climate model sensitivity studies. J. Geophys. Res. 89, 1267–1279.

Barron, E.J., Thompson, S., Hay, W.W., 1984. The potential of continental distribution as a climatic forcing factor. Nature 310, 574–575.

Barron, E.J., Hay, W.W., Thompson, S., 1989. The hydrologic cycle: a major variable during Earth history. Palaeogeogr. Palaeoclimatol. Palaeoecol. 75, 157–174.

Barron, E.J., Peterson, W.H., Thompson, S., Pollard, D., 1993. Past climate and the role of ocean heat transport: model simulations for the Cretaceous. Paleoceanography 8, 785–798.

Barron, E.J., Fawcett, P.J., Peterson, W.H., Pollard, D., Thompson, S.L., 1995. A "simulation" of mid-Cretaceous climate. Paleoceanography 10, 953–962.

Beck, R.A., Sinha, A., Burbank, D.W., Sercombe, W.J., Khan, A.M., 1999. Climatic, oceanographic, and isotopic consequences of the Paleocene India–Asia collision. In: Aubry, M.-P., Lucas, S.G., Berggren, W.A. (Eds.), Late Paleocene–early Eocene: Climatic and Biotic Events in the Marine and

Terrestrial Records. Columbia University Press, pp. 103–117.

Berner, R.A., 1994. GEOCARB II: a revised model of atmospheric $CO_2$ over Phanerozoic time. Am. J. Sci. 294, 56–91.

Bice, K.L., 1997. An investigation of Early Eocene Deep water warmth using uncoupled atmosphere and ocean general circulation models: model sensitivity to geography, initial temperatures, atmospheric forcing and continental runoff. Ph.D. Thesis, Pennsylvania State University, University Park, 363 pp.

Bice, K.L., Marotzke, J., 1999. Warm climate dynamics. Meeting Proceedings "Early Paleogene Warm Climates and Biosphere Dynamics", Swedish Geological Society, Goteborg, Sweden.

Bice, K.L., Barron, E.J., Peterson, W.H., 1997. Continental runoff and early Cenozoic bottom-water sources. Geology 25, 951–954.

Bice, K.L., Norris, R.D., Magno, E.A., 1999a. A new Cenomanian/Turonian equatorial temperature and its bearing on poleward heat transport. Eos 80, 492

Bice, K.L., Sloan, L.C., Barron, E.J., 1999b. Comparison of early Eocene isotopic paleotemperatures and the three-dimensional OGCM temperature field: the potential for use of model-derived surface water $\delta^{18}O$. In: Huber, B.T., MacLeod, K.G., Wing, S.L. (Eds.), Warm Climates in Earth History. Cambridge University Press, Cambridge, UK, pp. 79–131.

Broccoli, A.J., Manabe, S., 1992. The effects of orography on midlatitude northern hemisphere dry climates. J. Climate 5, 1181–1201.

Carissimo, B.C., Oort, A.H., Vonder Haar, T.H., 1985. Estimating the meridional energy transports in the atmosphere and ocean. J. Phys. Oceanogr. 15, 82–91.

Covey, C., Barron, E.J., 1988. The role of ocean heat transport in climatic change. Earth Sci. Rev. 24, 429–445.

Cowling, S.A., 1999. Plants and temperature: $CO_2$ uncoupling. Science 285, 1500–1501.

Cox, M.D., 1989. An idealized model of the world ocean. Part I: the global-scale water masses. J. Phys. Oceanogr. 19, 1730–1752.

Crowley, T.J., 1993. Climate change on tectonic time scales. Tectonophysics 222, 277–294.

Douglas, R.G., Savin, S.M., 1975. Oxygen and carbon isotope analyses of Tertiary and Cretaceous microfossils from Shatsky Rise and other sites in the north Pacific Ocean. Initial Rep. Deep Sea Drill. Proj. 32, 509–520.

Douglas, R.G., Woodruff, F., 1981. Deep-sea benthic foraminifera. In: Emiliani, C. (Ed.), The Sea vol. 7. Wiley-Interscience, New York, pp. 1233–1327.

Edmond, J.M., 1992. Himalayan tectonics, weathering processes and the strontium isotope record in marine limestones. Science 258, 1594–1597.

England, M.H., 1992. On the formation of Antarctic intermediate and bottom water in ocean general circulation models. J. Phys. Oceanogr. 22, 918–926.

Estes, R., Hutchison, J.H., 1980. Eocene lower vertebrates from

Ellesmere Island, Canadian Arctic Archipelago. Palaeogeogr. Palaeoclimatol. Palaeoecol. 30, 325–347.

Fawcett, P.J., Barron, E.J., 1998. The role of geography and atmospheric $CO_2$ in long term climate change: results from model simulations for the late Permian to the present. In: Crowley, T., Burke, K. (Eds.), Tectonic Boundary Conditions for Climate Reconstructions. Oxford University Press, pp. 21–36.

Flower, B.P., 1999. Warming without high $CO_2$? Nature 399, 313–314.

Freeman, K.H., Hayes, J.M., 1992. Fractionation of carbon isotopes by phytoplankton and estimates of ancient $CO_2$ levels. Global Biogeochem. Cycles 6, 185–198.

Gill, A.E., Bryan, K., 1971. Effects of geometry on the circulation of a three-dimensional southern-hemisphere ocean model. Deep-Sea Res. 18, 685–721.

Haq, B.U., Hardenbol, J., Vail, P.R., 1987. Chronology of fluctuating sea levels since the Triassic. Science 235, 1156–1167.

Hastenrath, S., 1982. On meridional heat transports in the world ocean. J. Phys. Oceanogr. 12, 922–927.

Kominz, M.A., 1984. Oceanic ridge volumes and sea level change: an error analysis. In: Schlee, J.S. (Ed.), Interregional Unconformities and Hydrocarbon Accumulation. American Association of Petroleum Geologists Memoir 36. AAPG, Tulsa, OK, pp. 109–127.

Kutzbach, J.E., Prell, W.L., Ruddiman, W.F., William, F., 1993. Sensitivity of Eurasian climate to surface uplift of the Tibetan Plateau. J. Geol. 101, 177–190.

Levitus, S., Burgett, R., Boyer, T.P., 1994. Salinity, NOAA Atlas NESDIS 3. World Ocean Atlas 1994 vol. 3. U.S. Government Printing Office, Washington, DC. 99 pp.

Mackensen, A., Ehrmann, W.U., 1992. Middle Eocene through Early Oligocene climate history and paleoceanography in the Southern Ocean: stable oxygen and carbon isotopes from ODP sites on Maud Rise and Kerguelen Plateau. Mar. Geol. 108, 1–27.

Maier-Reimer, E., Mikolajewicz, U., Crowley, T.J., 1990. Ocean general circulation model sensitivity experiment with an open central American isthmus. Paleoceanography 5, 349–366.

McKenna, M.C., 1980. Eocene paleolatitude, climate and mammals of Ellesmere Island. Palaeogeogr. Palaeoclimatol. Palaeoecol. 30, 349–362.

Mikolajewicz, U., Maier-Reimer, E., Crowley, T.J., Kim, K.-Y., 1993. Effect of Drake and Panamanian gateways on the circulation of an ocean model. Paleoceanography 8, 409–426.

Miller, K.G., Fairbanks, R.G., Mountain, G.S., 1987. Tertiary oxygen isotope synthesis, sea level history, and continental margin erosion. Paleoceanography 2, 1–19.

Norris, R.D., Jones, L.S., Corfield, R.M., Cartlidge, J.E., 1996. Skiing in the Eocene Uinta Mountains? Isotopic evidence in the Green River Formation for snow melt and large mountains. Geology 24, 403–406.

Otto-Bliesner, B.L., 1998. Effects of tropical mountain elevations on the climate of the Late Carboniferous; climate model simulations. In: Crowley, T., Burke, K. (Eds.), Tec-

tonic Boundary Conditions for Climate Reconstructions. Oxford University Press, pp. 100–115.

Pacanowski, R., Dixon, K., Rosati, A., 1993. The GFDL modular ocean users guide, GFDL Ocean Group Tech. Rep. 2.

Pagani, M., Freeman, K.H., Arthur, M.A., 1999. Late Miocene atmospheric $CO_2$ concentrations and the expansion of $C_4$ grasses. Science 285, 876–879.

Pearson, P.N., Palmer, M.R., 1999. Middle Eocene seawater pH and atmospheric carbon dioxide concentrations. Science 284, 1824–1826.

Raymo, M.E., 1991. Geochemical evidence supporting T.C. Chamberlin's theory of glaciation. Geology 19, 344–347.

Raymo, M.E., Ruddiman, W.F., 1992. Tectonic forcing of late Cenozoic climate. Nature 359, 117–122.

Raymo, M.E., Ruddiman, W.F., Froelich, P.N., 1988. Influence of late Cenozoic mountain building on ocean geochemical cycles. Geology 16, 649–653.

Reusch, D.N., Maasch, K.A., 1998. The transition from arc volcanism to exhumation, weathering of young Ca, Mg, Sr silicates, and $CO_2$ drawdown. In: Crowley, T., Burke, K. (Eds.), Tectonic Boundary Conditions for Climate Reconstructions. Oxford University Press, pp. 261–276.

Robin, G. de Q., 1988. The Antarctic ice sheet, its history and response to sea level and climatic changes over the past 100 million years. Palaeogeogr. Palaeoclimatol. Palaeoecol. 67, 31–50.

Rind, D., Chandler, M., 1991. Increased ocean heat transports and warmer climate. J. Geophys. Res. 96, 7437–7461.

Ruddiman, W.F., 1997. Tectonic Uplift and Climate Change. Plenum, New York. 535 pp.

Ruddiman, W.F., Kutzbach, J.E., 1990. Late Cenozoic uplift and climate change. Trans. R. Soc. Edinburgh Earth Sci. 81, 301–314.

Scotese, C.R., McKerrow, W.S., 1990. Revised world maps and introduction. In: Scotese, C.R., McKerrow, W.S. (Eds.), Palaeozoic Palaeogeography and Biogeography. Geological Society of London Memoir., 1–21.

Scotese, C.R., Ross, M.I., Schettino, A., 1998. Plate tectonic reconstruction and animation. Eos 79, 334.

Seidov, D., 1986. Numerical modelling of the ocean circulation and paleocirculation. In: Hsü, K.J. (Ed.), Mesozoic and Cenozoic Oceans. American Geophysical Union, Washington, DC, pp. 11–26.

Shackleton, N.J., Kennett, J.P., 1975. Paleotemperature history of the Cenozoic and the initiation of Antarctic glaciation: oxygen and carbon isotope analyses in DSDP Sites 277, 279, and 281. In: Kennett, J.P., Houtz, R.E., Andrew, P.B., Edwards, A.R. (Eds.), Initial Rep. Deep Sea Drill. Proj. 29, 743–755.

Shackleton, N.J., Hall, M.A., Boersma, A., 1984. Oxygen and carbon isotope data from Leg 74 foraminifers. Initial Rep. Deep Sea Drill. Proj. 74, 599–612.

Sloan, L.C., Barron, E.J., 1990. "Equable" climates during Earth history? Geology 18, 489–492.

Sloan, L.C., Rea, D.K., 1995. Atmospheric carbon dioxide and early Eocene climate: a general circulation modeling sensitivity study. Palaeogeogr. Palaeoclimatol. Palaeoecol. 119, 275–292.

Sloan, L.C., Walker, J.C.G., Moore, T.C., 1995. Possible role of ocean heat transport in early Eocene climate. Paleoceanography 10, 347–356.

Stocker, T.F., Wright, D.G., Mysak, L.A., 1992. A zonally averaged, coupled ocean-atmosphere model for paleoclimate studies. J. Climate 5, 773–797.

Stone, R.H., 1978. Constraints on dynamical transports of energy on a spherical planet. Dyn. Atmos. Oceans 2, 123–139.

Stott, L.D., Kennett, J.P., Shackleton, N.J., Corfield, R.M., 1990. The evolution of Antarctic surface waters during the Paleogene: inferences from the stable isotopic composition of planktonic foraminifers, ODP Leg 113. Proc. Ocean Drill. Program Sci. Results 113, 849–863.

Thompson, S.L., Pollard, D., 1997. Greenland and Antarctic mass balances for present and doubled $CO_2$ from the GENESIS version 2 global climate model. J. Climate 10, 871–900.

Toggweiler, J.R., Samuels, B., 1993. Is the magnitude of the deep outflow from the Atlantic Ocean actually governed by southern hemisphere winds? In: Heimann, M. (Ed.), The Global Carbon Cycle. Springer, New York, pp. 303–331.

Trenberth, K.E., 1979. Mean annual poleward energy transports by the oceans in the southern hemisphere. Dyn. Atmos. Oceans 4, 57–64.

Vail, P.R., Michum, R.M., Thompson, S., 1977. Seismic stratigraphy and global changes of sea level, part 4: global cycles of relative changes of sea level. In: Payton, C.E. (Ed.), Seismic Stratigraphy: Applications to Hydrocarbon Exploration. American Association of Petroleum Geologists Memoir 26. AAPG, Tulsa, OK, pp. 83–97.

Weaver, A.J., Aura, S.M., Myers, P.G., 1994. Interdecadal variability in an idealized model of the North Atlantic. J. Geophys. Res. 99, 12 423–12 441.

Zachos, J.C., Lohmann, K.C., Walker, J.C.G., Wise Jr, S.W., 1993. Abrupt climate change and transient climates during the Paleogene: a marine perspective. J. Geol. 101, 191–213.

Ziegler, A.M., Hulver, M.L., Rowley, D.B., 1997. Permian world topography and climate. In: Martini, I.P. (Ed.), Late Glacial and Postglacial Environmental Changes — Quaternary, Carboniferous–Permian and Proterozoic. Oxford University Press, New York, pp. 111–146.